Direct and indirect transition in $(GaAs)_n/(AlAs)_n$ superlattices with $n = 1-15$

H. Fujimoto,* C. Hamaguchi, T. Nakazawa, K. Taniguchi, and K. Imanishi†
Department of Electronic Engineering, Faculty of Engineering, Osaka University, Suita, Osaka 565, Japan

H. Kato and Y. Watanabe
Department of Physics, School of Science, Kwansei Gakuin University, Nishinomiya, Hyogo-ken 662, Japan
(Received 20 July 1989; revised manuscript received 17 November 1989)

Photoreflectance and photoluminescence measurements are carried out in $(GaAs)_n/(AlAs)_n$ superlattices with n ranged from 1 to 15 at room temperature. Analysis of photoreflectance spectra gives several critical-point energies with a high accuracy which coincide with the photoluminescence peak energies in superlattices with $n \geq 10$. In superlattices with $n < 10$ the lowest transition energy determined from photoreflectance analysis is found to be larger than the lowest peak energy of photoluminescence, whereas the higher-energy peak of photoluminescence agrees well with the transition energy obtained from the photoreflectance analysis. The present results strongly suggest an existence of crossover of direct and indirect transition in the superlattices around $n = 10$. Energy-band structures and momentum-matrix elements are calculated by tight-binding method based on sp^3s^* with including the second-nearest-neighbor interactions, which show a crossover of direct and indirect transition around $n = 8$. The lowest peak energies of photoluminescence data agree with the lowest calculated indirect band gaps in superlattices with $n < 10$ and with the lowest direct band gaps for $n \geq 10$. The lowest transition energies determined from the photoreflectance analysis exhibit a feature similar to the layer-number dependence of the calculated direct band gaps in the whole range of n, but a disagreement in the energy values between the two exists in the range of n from 5 to 10. A disagreement between the present and previous data for $n = 5$ is explained in terms of layer-number fluctuation, which is supported by the energy-band calculation of a long-period superlattice such as $(GaAs)_n/(AlAs)_n/(GaAs)_{n+1}/(AlAs)_n$.

I. INTRODUCTION

Electronic properties of heterostructures have received great interest because of their potential application to high-speed electron devices. Electrical and optical properties of two-dimensional electron gas confined in a quantum well region have been studied in detail and well explained by taking into account the singularity of the density of states.

Short-period superlattices (SL's) consisting of thin alternative layers have been investigated mainly in view of optical properties. However, fundamental questions remain unanswered regarding the fundamental absorption edge, direct, indirect, or pseudodirect transition. It is well known that the lowest conduction band of AlAs lies near the X point in the Brillouin zone, resulting in the indirect band gap, whereas the lowest conduction band of GaAs is located at the Γ point, resulting in the direct band gap. The Brillouin zone of the short-period SL's is folded in the direction of $\mathbf{k}$ vector perpendicular to the layer and thus it is expected that the lowest conduction band of $(GaAs)_1/(AlAs)_1$ SL becomes indirect or pseudodirect with the lowest state having predominantly the character of the folded X-point state.

Another concept of the band structure of $(GaAs)_n/(AlAs)_n$ SL's is the type-II band alignment due to the band crossing of the lowest Γ conduction band in GaAs and the lowest X conduction band in AlAs. Photoluminescence (PL) measurements are interpreted in terms of the type-II band alignment.[1-8] However, it should be noted that such a concept disregards the zone-folding effect and thus assumes electron-hole recombination across the AlAs barrier layers. Very recently Kato *et al.*[9] reported measurements of photoluminescence and absorption in the $(GaAs)_n/(AlAs)_n$ SL's at 14 K and found that the photoluminescence peak lies well below the fundamental absorption edge in the SL's with $n < 13$, suggesting the SL's are indirect band-gap materials.

From a theoretical point of view, the question of the electronic structure of $(GaAs)_n/(AlAs)_n$ SL's has been investigated by a variety of methods from the simplest Kronig-Penney calculation, through envelope-function-type calculations[10] to the sophisticated microscopic methods based on tight-binding,[11-17] empirical and self-consistent pseudopotential,[18-21] and local-density,[22-24] or augmented-spherical-wave calculations.[25] These results are contradictory and the crossover of the direct or indirect band gap depends on the model. For example, Nakayama and Kamimura,[26] using a self-consistent pseudopotential method, predicted that only the $(GaAs)_1/(AlAs)_1$ SL has its lowest conduction-band state at the R point in the SL Brillouin zone, while the lowest conduction-band state of the $(GaAs)_n/(AlAs)_n$ SL's with $n = 2$, 3, and 4 is predominantly Γ-like in character, resulting in a direct energy gap. In contrast, Andreoni and Car,[27] using a non-self-consistent, supercell, empirical pseudopotential method, have shown that the band gaps of the $n = 1$, 2, 3, and 4 SL's are pseudodirect with the

lowest state having predominantly the character of the folded X-point state. Yamaguchi,[14] using the tight-binding method, has shown that the conduction-band state of $n=1$, 2, 3, 4, and 5 is indirect with the lowest state at the X point, while the conduction-band state of $n=7-20$ is direct. We have shown that a combination of photoreflectance (PR) and PL measurements gives good information about the direct-indirect crossover in the $(GaAs)_m/(AlAs)_5$ SL's with m ranging from 3 to 11, where the crossover occurs at around $m=7$ in the $(GaAs)_m/(AlAs)_5$ SL's. In addition we found from the energy-band calculations based on the tight-binding method that the lowest-energy gap at the Γ point is optically forbidden or pseudodirect for $m<5$, reflecting the zone-folding effect. These investigations have been carried out in the SL's with fixed AlAs layer number $[(GaAs)_m/(AlAs)_5]$.

In this paper we will report photoreflectance and photoluminescence measurements in the $(GaAs)_n/(AlAs)_n$ SL's which are grown very carefully in the range $n=1-15$. We found that the crossover of the direct and indirect transitions occurs at about $n=10$. We compare the experimental results with the energy-band calculations based on the tight-binding method, where we find a reasonable agreement with each other, supporting an existence of the crossover of the direct and indirect band gap. In the present work we observed the transition energies, determined from the analysis of photoreflectance data for the $(GaAs)_5/(AlAs)_5$ SL, differ from those reported previously. We discuss the difference in this paper. In Sec. II we describe experimental procedures and results. We also present analysis of photoreflectance data and compare with photoluminescence data in Sec. II. In Sec. III we present theoretical calculations of energy-band structure using the tight-binding method, where we will discuss direct allowed and forbidden transitions, and then compare the results with the experimental data. Discussion of the present results is given in Sec. IV. As stated above we found a difference between the present and previous experimental data, which will be discussed in terms of long-period superlattices. The speculation about the long-period superlattices arises from the difficulty in keeping exact periodicity during the growth. We found that this idea explains the difference observed in our experiments. Finally we summarize the present results.

II. EXPERIMENTAL PROCEDURES AND RESULTS

The set of 15 samples used in the present work were epitaxially grown at 570 °C on (100) semi-insulating GaAs substrates by molecular-beam epitaxy (MBE). The values of n were 1–15 and the multiple layers were 200 periods. The layer thicknesses of GaAs and AlAs were accurately controlled by monitoring the period of the intensity oscillation of a specularly reflected beam in a reflection high-energy electron diffraction (RHEED) pattern.[28] The thickness of the individual atomic layers of the SL's has been confirmed by x-ray diffraction measurements as reported previously.[29] The experimental arrangement used in the present work is reported elsewhere[30] and shown schematically in Fig. 1, which is similar to those used by

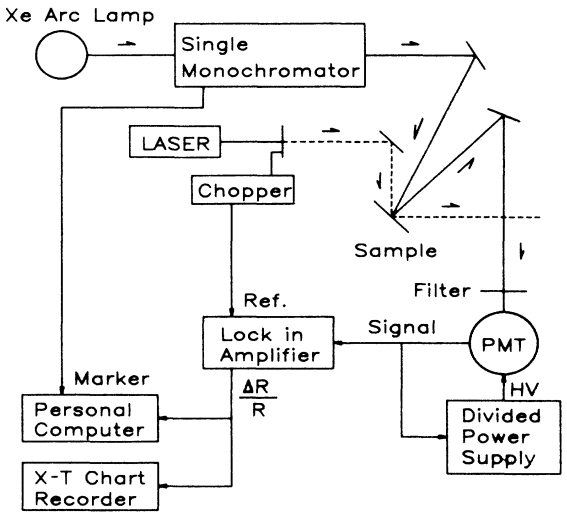

FIG. 1. Schematic diagram of the PR setup. The laser beam is chopped at a frequency of 210 Hz. The signal is detected by a photomultiplier tube and processed by a lock-in amplifier and a personal computer.

Glembocki et al.[31,32] and Shay.[33] Their function consists of four elements; modulation, optics, detection, and data storage. The modulation is accomplished by mechanically chopping a laser of photon energy greater than the band gap of the sample. The reflectance measurement is performed with a probe beam of white light dispersed by a monochromator. The light beam reflected from the sample surface is passed through a filter which blocks the laser light and is detected by a photomultiplier tube (PMT). The signals from the PMT are amplified by a lock-in amplifier tuned to the modulation frequency of the chopper. An electric servo mechanism on the high-voltage power supply of the PMT (divided power supply) is used to maintain a constant dc voltage across the load resistance of the PMT, allowing us to obtain the ratio $\Delta R/R$ directly.[34] The digitized data are recorded by a personal computer. Data analysis was carried out by a Hewlett-Packard computer (HP9000 model 550). In our system, we used a 500-W Xe arc lamp for a light source of the probe light and a 50-cm single monochromator of JASCO CT-50S with a 1200-lines/mm grating blazed at 750 nm. The intensity of the Ar-ion laser, at 488.0 or 476.5 nm, for modulation chopped at 210 Hz was reduced to about 0.2 mW by using neutral density filters. For PL measurements, the samples were excited with about 1 W of the 488.0-nm line of the Ar-ion laser and luminescence spectra were analyzed with an 80-cm-focal-length double monochromator (SPEX Industries, Inc. model 1401).

Since the experimental data of PR are anlayzed by the third-derivative formula derived by Aspnes and Rowe[35,36] we discuss the formulation here. The theoretical expression for the modulated reflectance in the presence of the electric field perturbation involves both the real and imaginary parts of the complex dielectric function ϵ. For normal incidence, the change in the reflectance, ΔR, has the form

$$\Delta R/R = \alpha \Delta\epsilon_1 + \beta \Delta\epsilon_2 , \quad (1)$$

where $\Delta\epsilon = \Delta\epsilon_1 + i\Delta\epsilon_2$ is the perturbation-induced change in ϵ, and α and β are the Seraphin coefficients which are a function of ϵ_1 and ϵ_2.[37] A detailed discussion on calculating $\Delta\epsilon$ and its effects on the line shape are given by Aspnes.[36] The modulated reflectance spectrum in the region of weak electric field is well expressed by the following line-shape formula derived by Aspnes:

$$\Delta R/R = \sum_j^p \mathrm{Re}[C_j \exp(i\theta_j)(E - E_{gj} + i\Gamma_j)^{-m_j}] , \quad (2)$$

where p is the number of critical points, E the photon energy, C_j, θ_j, E_{gj}, and Γ_j are the amplitude, phase, energy gap, and broadening parameter, respectively, of the jth critical point. The value of m_j is a parameter which depends on the critical-point type, $m_j = 3.5$, 3.0, and 2.5 for the one-, two-, and three-dimensional critical points, respectively. The energy gap and the broadening parameters are determined by fitting the line shape of Eq. (2) to the experimental data. The best-fit procedure was performed by using the method proposed by Rosenbrock.[38] For the best fit, we have to determine the dimensionality

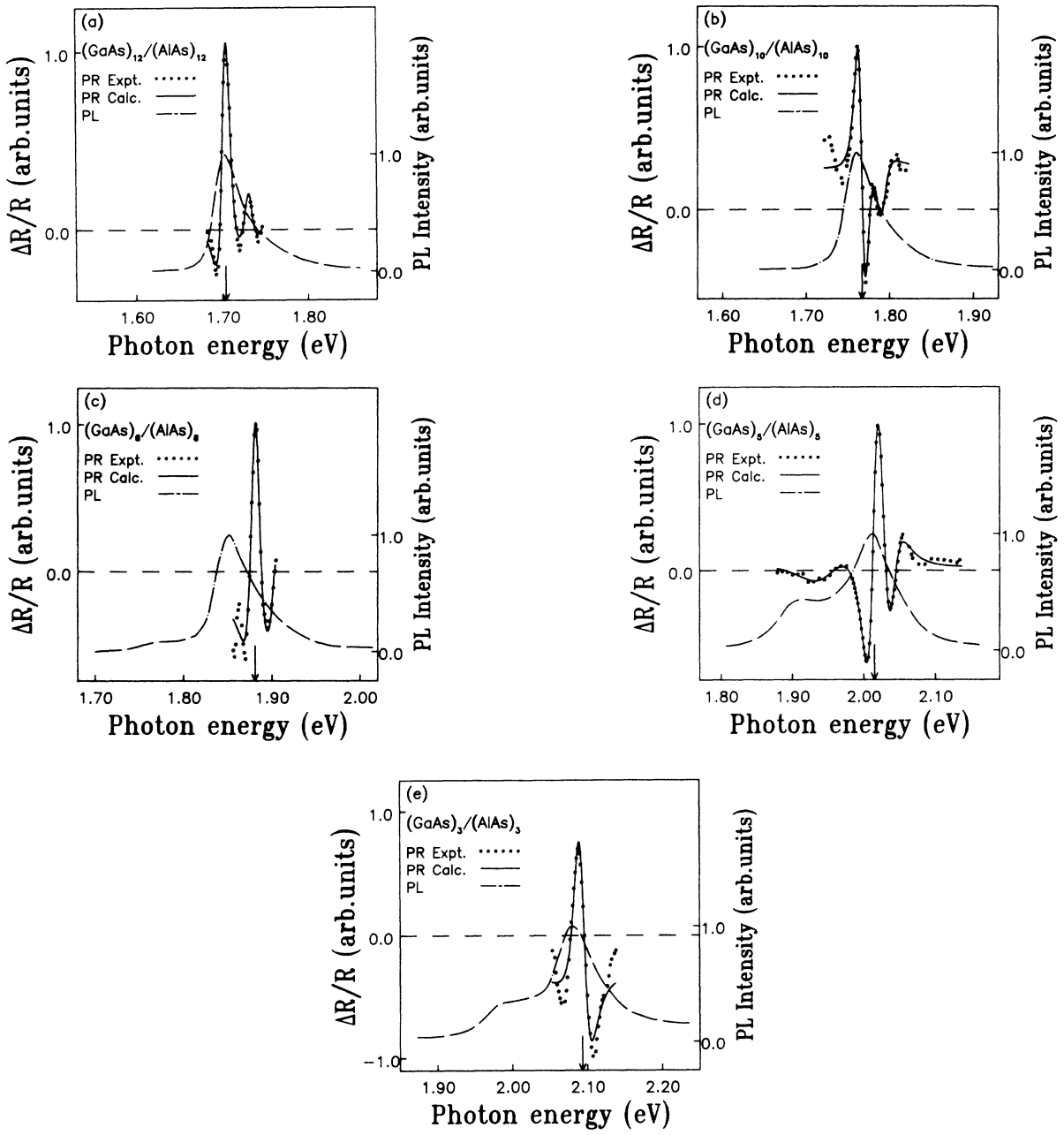

FIG. 2. Room-temperature PR (open circles) and PL (dot-dashed curve) experimental spectra for (a) $(GaAs)_{12}/(AlAs)_{12}$, (b) $(GaAs)_{10}/(AlAs)_{10}$, (c) $(GaAs)_8/(AlAs)_8$, (d) $(GaAs)_5/(AlAs)_5$, and (e) $(GaAs)_3/(AlAs)_3$ SL samples. The solid curve is determined by fitting the line shape of Eq. (2) to the PR experimental spectrum. Representative values of PR data are picked up and plotted in order to avoid a complexity. The vertical arrow indicates the lowest interband transition energy obtained by the fitting procedure.

of the critical points. It may be expected that the critical points of the SL's with thick barriers (large value of n) are two dimensional due to localization of the wave functions in the well regions (GaAs regions), while those with thin barriers (small value of n) are three-dimensional because of the extended nature of the wave functions. We carried out the best-fit analysis by using $m_j=2.5$ (three dimensional) and 3 (two dimensional), and found that the obtained critical-point energies are almost the same. In the present work, therefore, the experimental data of PR are analyzed by using Eq. (2) with $m_j=2.5$ (three-dimensional critical point). A theoretical analysis of PR line shape has been reported by Glembocki and Shanabrook.[39] Their results indicate that PR signals of quantum well structures where electrons and holes are confined in the well region are to be analyzed by the first-derivative formula. In the samples used in the present work, however, electrons and holes are extended in the superlattice and thus we have a three-dimensional-like situation, similar to the bands of a bulk material. This is correct when the applied electric field is low. At high electric fields, the localization of electron and hole wave functions and the formation of stark ladders occur.[40–44] This kind of localization appears in superlattices with a specific well and barrier widths.[40–44] In the present experiments we carried out PR measurements at different excitation intensities and no change in the critical points was observed, which indicates that such a localization effect is not present in the present experiments.

Figure 2(a) shows room-temperature PR (open circles) and PL (dot-dashed curve) experimental spectra together with the best-fit PR spectra (solid curve) by using Eq. (2) for the $(GaAs)_{12}/(AlAs)_{12}$ SL, where the vertical arrow indicates the lowest interband transition energy obtained by the fitting procedure. We find in Fig. 2(a) that the lowest transition energy of PR, 1.704 eV, is in good agreement with the peak position of the PL. Although the PR spectra show complicated structures arising from combination of two different critical points (or more than two in other SL's), the best-fit curve agrees well with the experimental curve. It is very important to point out in Fig. 2(a) that the PR spectrum shows a sharp structure at room temperature where the PL spectrum is very broad. Similar results are obtained for the $(GaAs)_n/(AlAs)_n$ with $n=10-15$. For the sake of later discussion we present the results for $n=10$, 8, 5, and 3 in Figs. 2(b), 2(c), 2(d), and 2(e), respectively, where the open circles are the experimental PR data, the solid curve is best fit to the experimental PR data (the vertical arrow is the lowest transition energy), and the dot-dashed curve is the PL data.

It is clearly seen in Figs. 2(a) ($n=12$) and 2(b) ($n=10$) that the lowest critical-point energies obtained from the PR are very close to the photon energies corresponding to the PL peaks. Therefore we can conclude that the SL's with $n>10$ have direct energy gaps. On the other hand, optical properties of the SL's with $n<10$ exhibit quite different features compared to those for $n>10$. We find in Fig. 2(c) for the $n=8$ SL that the lowest transition energy, 1.881 eV, obtained by the best-fit procedure of the PR spectrum (indicated by the vertical arrow) is higher than the PL peak energy, 1.85 eV. Similar results

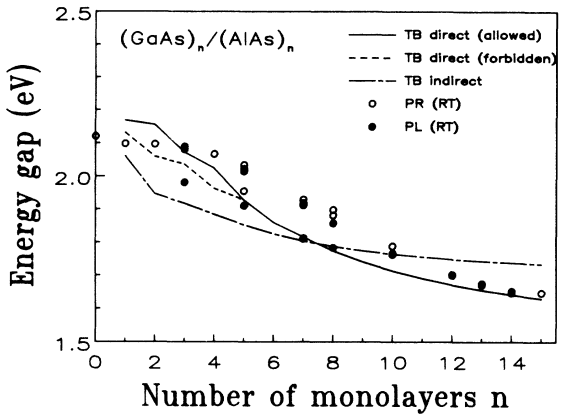

FIG. 3. Transition energies of the $(GaAs)_n/(AlAs)_n$ SL's, where the solid, dashed, and dot-dashed curves represent the lowest direct (allowed), the lowest direct (forbidden), and the lowest indirect transition energies, respectively, and the open and solid circles are the energies determined from the PR and the PL measurements, respectively.

are obtained for the SL's with $n=5$ and 3, which are shown in Figs. 2(d) and 2(e), respectively. It is very important to point out in Figs. 2(d) ($n=5$) and 2(e) ($n=3$) that the lowest direct transition energy determined from the PR analysis is located higher than the low-energy threshold of PL, where the PL exhibits a weak shoulder at about 1.91 eV and a peak at about 2.01 eV for $n=5$ and a shoulder at about 1.98 eV and a peak at about 2.08 eV for $n=3$. It is very interesting to point out that the high-energy peak of the PL coincides with the lowest direct transition energy determined from the PR analysis, indicating that the PL peak arises from the direct recombination. We found that the PL intensity of the SL's with $n<10$ is very weak compared with those of the SL's with $n>10$. These results strongly suggest that the $(GaAs)_n/(AlAs)_n$ SL's with $n<10$ are indirect and that the crossover of the direct and indirect transition occurs around $n=10$.

The lowest transition energy determined from the PR spectra is plotted in Fig. 3 as a function of the number of layers n by the open circle, together with PL peak energy (solid circle), where we find that the lowest PR transition energies and PL peak energies decrease monotonically with increasing the number of layers n, and the lowest PL peak energies are lower than the PR transition energies for $n<10$. The higher PL peak energies observed in the SL's with $n<10$ agree well with the PR transition energies. The solid, dot-dashed, and dotted curves are the energies of the direct allowed, direct forbidden, and indirect transitions, calculated from the tight-binding method which will be discussed in the next section in detail. These experimental and calculated values are also tabulated in Table I, where the value in the parentheses is the lowest direct forbidden transition energy calculated from the tight-binding method. We find in Fig. 3 that a reasonable agreement exists in the feature of direct and indirect crossover between the experimental and calculated results.

TABLE I. Transition energies obtained from the PR and PL measurements at room temperature, together with the direct allowed transition energies calculated by the tight-binding method. The energies in parentheses are the forbidden transitions.

	PR (eV)		PL (eV)		Tight-binding (eV)		
n	E_{g_1}	E_{g_2}	E_{g_1}	E_{g_2}	E_{t_1}	E_{t_2}	E_{t_3}
1	2.120				(2.061)	(2.156)	2.168
2	2.097				(2.060)	(2.084)	2.151
3	2.099		1.981	2.082	(2.037)	2.069	(2.078)
4	2.067				(1.963)	2.022	(2.082)
5	2.015	2.035	1.910	2.023	1.927	(1.932)	(2.000)
7	1.918	1.929	1.812	1.912	1.815	(1.856)	(1.903)
8	1.881	1.898	1.783	1.857	1.773	(1.832)	(1.859)
10	1.766	1.788	1.762		1.712	(1.789)	(1.795)
12	1.704	1.732	1.700		1.671	(1.712)	(1.835)
13	1.675		1.680		1.654	(1.763)	(1.821)
14	1.652		1.647		1.641	(1.756)	(1.804)
15	1.647				1.629	(1.749)	(1.796)

We have to note here that the present experimental data for the SL $(GaAs)_5/(AlAs)_5$ differ from those reported in our previous paper.[30] The lowest transition energies obtained from the analysis of PR spectra and PL peak energy in $(GaAs)_m/(AlAs)_5$ with $m=5$ are 1.947 and 1.905 eV, respectively. On the other hand, the present results show that the lowest transition energies of PR spectra and PL peak energy are 2.02 and 1.91 eV, respectively. The difference may be explained in terms that a monolayer fluctuation of GaAs results in a considerable difference in the energy gaps, which will be shown later by the tight-binding calculation of the energy-band structures. The samples used in our previous work were grown at Fujitsu Laboratories by MBE, and the layer numbers of GaAs and AlAs are controlled by keeping the growth rate and time constant. Therefore the fluctuation of the layer number is inevitable. The samples used in the present work were grown by monitoring the RHEED pattern oscillation and the layer numbers are checked by using x-ray diffraction method, which revealed that the samples have high quality of periodicity.

III. ENERGY-BAND CALCULATIONS OF SUPERLATTICES

In our previous paper[30] we reported that the experimental data of the photoluminescence and photoreflectance are well explained by the energy-band structure calculated by the tight-binding method. In addition we have shown that the lowest direct band gap of the $(GaAs)_m/(AlAs)_5$ SL's with $m<5$ is a forbidden gap due to the zone-folding effect. The experimental results exhibit good agreement with the calculations. However, such a good agreement seems to be accidental, because the periodicity of the atomic layers is not so strict and fluctuation of the periodicity results in a change in the energy gaps. Another important thing is that such energy-band calculations are carried out at 0 K without taking into account the temperature dependence. We discussed the temperature dependence of the energy-band structure in bulk III-V semiconductors by using the pseudopotential method,[45] but in this paper we will not discuss the temperature dependence because of the complexity of the effect. In the following we summarize the method of the tight-binding theory and analysis of the momentum-matrix elements for the optical transitions.

The present calculations of the SL energy bands are carried out by the method used by Yamaguchi,[14] where the sp^3s^* tight-binding method proposed by Vogl *et al.*[46] has been extended to the case of the SL's including the second-nearest-neighbor interactions[47] in addition to the nearest-neighbor interactions. The diagonal matrix elements and the values of the nearest and second-nearest interactions used in the present calculations are those of Yamaguchi.[14] Another parameter we have to determine is the energy-band discontinuity. The valence-band discontinuity is estimated to be 0.54 eV from a comparison of the transition energies between the experimental (PR and PL) data and theoretical (tight-binding method) calculations.[30,48]

In this paper, we will present energy-band calculations of the $(GaAs)_n/(AlAs)_n$ SL's with $n=1-15$ and discuss the optical transitions in detail. For this purpose, we describe the momentum-matrix elements between the

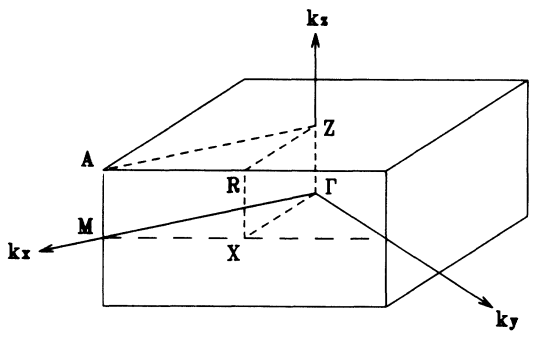

FIG. 4. The Brillouin zone of the superlattice folded along the z direction.

valence and conduction bands at the Γ point. We define the momentum-matrix elements by

$$M_x = \sum_{b,n,n'} \langle n',b|C_{bn'}P_xC_{bn}|n,b\rangle \ , \tag{3}$$

where $|n,b\rangle$ ($|n',b\rangle$) is the atomic function with atomic index b and atomic orbitals n (n') ($=s$, p_x, p_y, p_z, and s^*), C_{bn} and $C_{bn'}$ are the coefficients for the functions $|n,b\rangle$ and $|n',b\rangle$, respectively, and P_x is the x component of the momentum operator, where we assumed that the incident light is polarized parallel to the layers because the light is incident along the growth direction. We use a zinc-blende-structure tight-binding Hamiltonian[14,46,47] for the basis of quasiatomic functions localized in the unit cell at $\mathbf{R}_i$, $|n,b,\mathbf{R}_i\rangle$. The Bloch-type tight-binding states are

$$|n,b,\mathbf{k}\rangle = \frac{1}{\sqrt{N}} \sum_i \{\exp[i(\mathbf{k}\cdot\mathbf{R}_i + \mathbf{k}\cdot\mathbf{V}_b)]\}|n,b,\mathbf{R}_i\rangle \ , \tag{4}$$

where quantum numbers n run over the s, p_x, p_y, p_z, and s^* (that is, excited s) orbitals. The N wave vectors $\mathbf{k}$ lie in the first Brillouin zone. The site index b is either a (for anion) or c (for cation). The anion positions are $\mathbf{R}_i$ and the cation positions are $\mathbf{R}_i+\mathbf{V}_b$ with $\mathbf{V}_b=\delta_{c,b}(a_L/4)(1,1,1)$ and with a_L being the lattice constant. The quasiatomic functions are Löwdin orbitals, which are symmetrically orthogonalized atomic orbitals. The Schrödinger equation for the Bloch function $|\mathbf{k},\lambda\rangle$ is

$$[H - E(\mathbf{k},\lambda)]|\mathbf{k},\lambda\rangle = 0 \ , \tag{5}$$

or, in this basis

$$\sum_{m,b'} [\langle n,b,\mathbf{k}|H|m,b',\mathbf{k}\rangle - E(\mathbf{k},\lambda)\delta_{n,m}\delta_{b,b'}] \times \langle m,b',\mathbf{k}|\mathbf{k},\lambda\rangle = 0 \ . \tag{6}$$

The solutions are

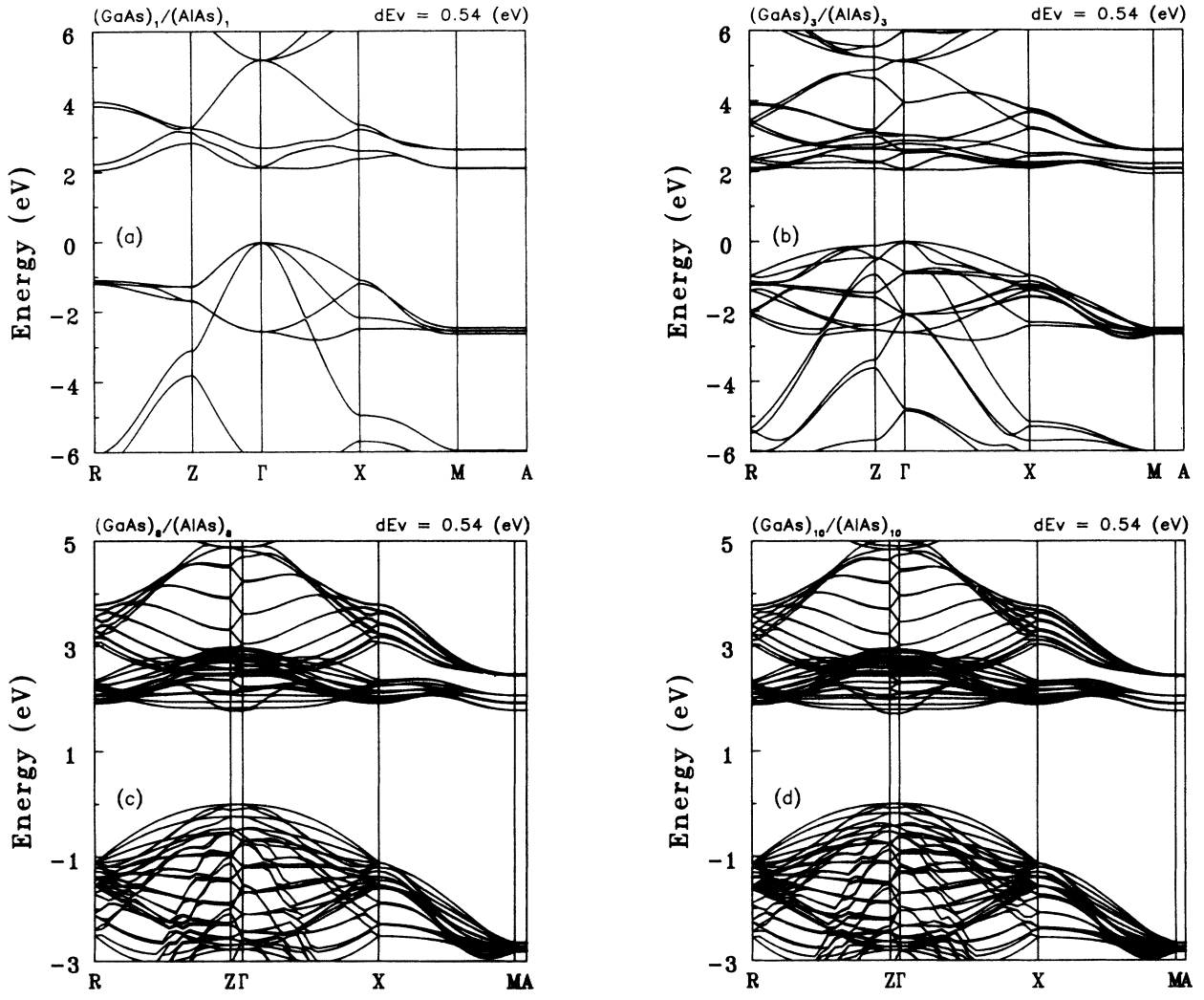

FIG. 5. Energy-band structures of $(GaAs)_n/(AlAs)_n$ SL's calculated by the tight-binding method. (a) $(GaAs)_1/(AlAs)_1$, where the top valence band is at the Γ point and the lowest conduction band is at the R point in the Brillouin zone; (b) $(GaAs)_3/(AlAs)_3$, where the top valence band is at the Γ point and the lowest conduction band is at the M point in the Brillouin zone; (c) $(GaAs)_8/(AlAs)_8$, where the top valence band is at the Γ point and the lowest conduction band is at the Γ point in the Brillouin zone; and (d) $(GaAs)_{10}/(AlAs)_{10}$, where the top valence band is the Γ point and the lowest conduction band is at the Γ point in the Brillouin zone.

$$|\mathbf{k},\lambda\rangle=\sum_{n,b}|n,b,\mathbf{k}\rangle\langle n,b,\mathbf{k}|\mathbf{k},\lambda\rangle\ , \tag{7}$$

where the band index λ has 10 $(n+n)$ values for the SL's $(GaAs)_n/(AlAs)_n$. Diagonalization of the Hamiltonian in this $|n,b,\mathbf{k}\rangle$ basis gives eigenvalues (energy bands) and eigenvectors (wave functions). Calculation of the momentum-matrix elements defined by Eq. (3) is straightforward. It is evident from the symmetry consideration of the SL's that the momentum-matrix elements M_x and M_y are identical, and therefore we calculated M_x only.

IV. DISCUSSION

The first Brillouin zone and the notation of the zone edges are illustrated in Fig. 4, where the Brillouin zone of a SL is folded in the z direction and the Z point is given by $2\pi/a_L(0,0,1/(m+n))$ for $(GaAs)_m/(AlAs)_n$ with a_L the lattice constant. The energy-band structures of the $(GaAs)_n/(AlAs)_n$ SL's for $n=1$, 3, 8, and 10 are shown in Figs. 5(a), 5(b), 5(c), and 5(d), respectively. The energy-band structures are calculated assuming that the valence-band discontinuity is 0.54 eV as reported in the previous paper.[30] The lowest conduction band appears at the R point $(n=1)$, and M point $(n=2,3,4,5,6,$ and $7)$ resulting in indirect band gap, and at the Γ point for $n>7$, giving rise to direct band gap.

In order to clarify the allowed and forbidden transitions we carried out calculations of momentum-matrix elements and the results, squared momentum-matrix element versus layer number n, are shown in Fig. 6, where the notation v_1-c_j stands for the optical transition between the top valence band and lowest jth conduction band (c_j) at the Γ point. Since we do not know the relative strength of the momentum-matrix element between different atoms, we assumed that the contribution from different atoms is the same. This may be understood from the following fact. In III-V compound semiconductors such as GaAs, AlAs, and GaP, the momentum-matrix elements between valence band and conduction band $(P=\langle\Gamma_2'|P_x|\Gamma_{25}'\rangle)$ are almost independent of the materials,[49] and therefore matrix elements such as $\langle s,\mathrm{Ga}|P_x|p_x,\mathrm{Ga}\rangle$, $\langle s,\mathrm{As}|P_x|p_x,\mathrm{As}\rangle$, and so on are almost constant. Then we calculated the momentum-matrix elements and obtained the summation of the squared momentum-matrix elements which is normalized by the values for bulk GaAs. These normalized values are plotted in Fig. 6. We find in Fig. 6 that the transition between the top valence band and the lowest conduction band is forbidden for the $(GaAs)_n/(AlAs)_n$ SL's with $n=1$ and 3, and very weak for $n=2$ and 4. On the other hand, the optical transition between the top valence band and the second lowest conduction band is allowed for these SL's $(n=1-4)$. The lowest allowed and forbidden direct band-gap energies are plotted by the solid curve and dot-dashed curve, respectively, in Fig. 3, along with the lowest indirect band-gap energies by the dotted curve. As stated in the preceding section the overall features of the layer-number dependence and the crossover of the direct and indirect band gaps are in a reasonable agreement with the present observation, although the calculated energy gaps lie a little bit lower than the experimentally determined gaps in the region of $n=5-10$. Noting the fact that the energy gaps depend on temperature and on the valence-band discontinuity, the agreement is rather excellent. We find in Fig. 3 that the tight-binding calculations give the crossover of the direct and indirect transition at around $n=8$. The calculated lowest gaps exhibit a good agreement with the PL peak energies. These results strongly suggest that the $(GaAs)_n/(AlAs)_n$ SL's exhibit crossover of the direct and indirect transition in the region of n about 10.

Now, we discuss the difference between the present work and the previous work in the $(GaAs)_5/(AlAs)_5$ SL.

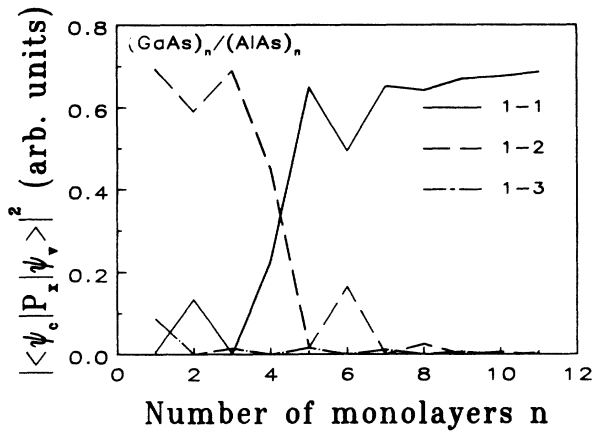

FIG. 6. Squared momentum-matrix elements of the $(GaAs)_n/(AlAs)_n$ SL's are plotted as a function of GaAs monolayers n, where the notation 1-n $(n=1,$ 2, and 3) stands for the values between the top valence bands and the nth conduction band, respectively.

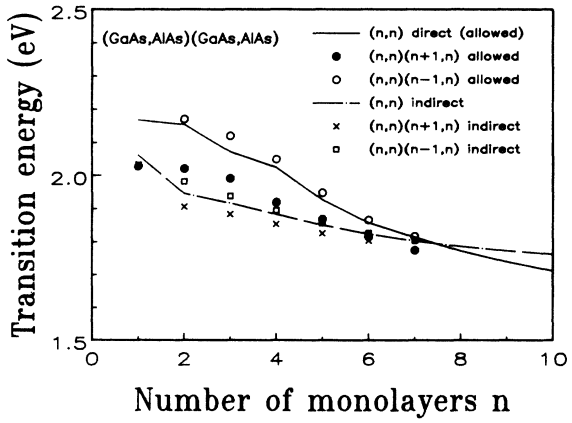

FIG. 7. Transition energies of long-period SL's are shown as a function of atomic layer number n, along with transition energies for normal SL's (n,n). Notations (n,n) and $(n,n)(n+1,n)$ stand for SL's $(GaAs)_n/(AlAs)_n$ and $(GaAs)_n/(AlAs)_n/(GaAs)_{n+1}/(AlAs)_n$, respectively. Solid and dot-dashed curves are the energy gaps of the lowest direct allowed transition and the lowest indirect transition for SL's (n,n), respectively. Solid and open circles are the lowest allowed transition energy for $(n,n)(n+1,n)$ and $(n,n)(n-1,n)$, respectively. Crosses and squares represent the lowest indirect gap for $(n,n)(n+1,n)$ and $(n,n)(n-1,n)$, respectively.

The difference in the transition energy determined from the PR and the PL peak energy in the SL is about 60 meV, which is beyond the range of experimental errors. One of the most probable origins of the difference may be due to the fluctuation of the layer number during the process of SL growth. A change of the layer number results in a change in the energy gaps which is evident from the layer-number dependence of the gaps shown in Fig. 3. In order to discuss this effect we will try to calculate energy-band structure of a long-period superlattice such as $(GaAs)_n/(AlAs)_n/(GaAs)_{n+1}/(AlAs)_n$. In this paper we define such a long-period superlattice as $(n,n)(n+1,n)$ SL. We carried out energy-band calculations of $(n,n)(n+1,n)$, $(n,n)(n-1,n)$, $(n,n)(n,n+1)$, and $(n,n)(n,n-1)$ SL's. The matrix elements of the tight-binding Hamiltonian for the $(n,n)(n+1,n)$ SL are easily obtained by extending Eq. (4) from $(GaAs)_n/(AlAs)_n$ basis into $(GaAs)_n/(AlAs)_n/(GaAs)_{n+1}/(AlAs)_n$ basis.

The calculated results for these long-period SL's are shown by solid and open circles for the lowest direct band gaps of $(n,n)(n+1,n)$ and $(n,n)(n-1,n)$, respectively, and by crosses and open squares for the lowest indirect band gaps, respectively, in Fig. 7, where the lowest allowed and indirect band gaps of the $(GaAs)_n/(AlAs)_n$ SL's [(n,n) SL] are plotted by the solid and dot-dashed curve, respectively, for comparison.

It is very interesting to point out that the lowest direct band gap depends on the layer number of GaAs. This may be understood by taking into account the fact that the lowest conduction band reflects the character of GaAs. It is evident from the results shown in Fig. 7 that a monolayer fluctuation of GaAs results in about a 50–80-meV shift in the energy gaps. The shift is comparable with the difference in the energy gaps of the $(GaAs)_5/(AlAs)_5$ SL between the present and the previous work. Although the samples used in the present work were grown by monitoring the RHEED oscillations, the monitored area is limited and fluctuation of the layer periods in the plane is inevitable. The fluctuation of the superlattices in the plane was not investigated systematically. However, some experimental results indicate the existence of such a fluctuation. For example, the broadening parameters were found to be almost independent of temperature, which may be interpreted in terms that the broadening is dominated by such a fluctuation, in the plane. This also results in the difference in the transition energies between different samples with the same period.

The present work is summarized as follows. We carried out photoreflectance and photoluminescence measurements in the $(GaAs)_n/(AlAs)_n$ superlattices at room temperature and found that photoluminescence peak energy (lowest band) is lower than transition energy determined from photoreflectance analysis for the SL's with $n < 10$, whereas these energies coincide with each other for the SL's with $n \geq 10$. These results indicate that the SL's have indirect band gap for $n < 10$ and direct band gap for $n \geq 10$ at room temperature. Energy-band calculations based on the tight-binding method have been performed in the SL's of $(GaAs)_n/(AlAs)_n$. Using the eigenfunctions obtained from the tight-binding calculations, we estimated the momentum-matrix elements to clarify the selection rule of the optical transitions near the fundamental absorption edge. The matrix elements between the top valence bands and the lowest three conduction bands reveal that the lowest transition for the SL with $n = 5$ is forbidden, resulting from the band folding effect. When we take into account the selection rule, it is found that the transition energy determined from the photoreflectance measurements shows a good agreement with the calculated transition energy except SL's with n from 5 to 10. The present calculations show that the SL's of $(GaAs)_n/(AlAs)_n$ exhibit a crossover of the direct and indirect transitions around $n = 8$, as reported by Yamaguchi.[14] We found a difference in the transition energy between the present and previous work for the case of $(GaAs)_5/(AlAs)_5$. The difference is explained in terms of the fluctuation of the atomic layer number n. This speculation is supported by theoretical calculation of the energy-band structure by taking into account the fluctuation, where we carried out energy-band calculations of a long-period superlattice such as $(GaAs)_n/(AlAs)_n/(GaAs)_{n+1}/(AlAs)_n$. We found from these calculations that the energy bands are predominantly determined by the layer number $(n+1)$ of GaAs.

Finally we would like to point out that the PR spectra exhibit a very weak structure around the indirect gap as seen in Fig. 2(d) [at about 1.91 eV in the $(GaAs)_5/(AlAs)_5$ SL]. The structure appears reproducibly and exceeds the range of error in our experiment. As seen in Fig. 3, the corresponding energy is very close to the forbidden gap and thus one of the most probable possibilities for the origin of the structure may be due to the forbidden transition. We are now carrying out these experiments at low temperatures, placing main interest in the temperature dependence of the transition energies. The results will be published in the future.

---

*Permanent address: Research and Development Center, Toshiba Corporation, Saiwai-ku, Kawasaki-shi, Kanagawa-ken 210, Japan.

†Permanent address: Fujitsu Laboratories, Ltd., Atsugi-shi Kanagawa-ken 243-01, Japan.

[1]E. Finkman, M. D. Sturge, and M. C. Tamargo, Appl. Phys. Lett. **49**, 1299 (1986).

[2]E. Finkman, M. D. Sturge, M.-H. Meynadier, R. E. Nahory, M. C. Tamargo, D. M. Hwang, and C. C. Chang, J. Lumin. **39**, 57 (1987).

[3]G. Danan, B. Etienne, F. Mollot, and R. Planel, Phys. Rev. B **35**, 535 (1987).

[4]F. Minami, K. Hirata, K. Era, T. Yao, and Y. Masumoto, Phys. Rev. B **36**, 2875 (1987).

[5]D. S. Jiang, K. Kelting, H. J. Queisser, and K. Ploog, J. Appl. Phys. **63**, 845 (1988).

[6]K. Takahashi, T. Hayakawa, T. Suyama, M. Kondo, S. Yamamoto, and T. Hijikata, J. Appl. Phys. **63**, 1729 (1988).
[7]K. J. Moore, P. Dawson, and C. T. Foxon, Phys. Rev. B **38**, 3368 (1988).
[8]K. J. Moore, G. Duggan, P. Dawson, and C. T. Foxon, Phys. Rev. B **38**, 5535 (1988).
[9]H. Kato, Y. Okada, M. Nakayama, and Y. Watanabe, Solid State Commun. **70**, 535 (1989).
[10]G. Bastard, Phys. Rev. B **25**, 7584 (1982).
[11]S. Nara, Jpn. J. Appl. Phys. **26**, 1713 (1987).
[12]S. Nara, Jpn. J. Appl. Phys. **26**, 690 (1987).
[13]J. N. Schulman and T. C. McGill, Phys. Rev. B **19**, 6341 (1979).
[14]E. Yamaguchi, J. Phys. Soc. Jpn. **56**, 2835 (1987).
[15]J. Ihm, Appl. Phys. Lett. **50**, 1068 (1987).
[16]K. K. Mon, Solid State Commun. **41**, 699 (1982).
[17]W. A. Harrison, Phys. Rev. B **23**, 5230 (1981).
[18]Jian-Bai Xia, Phys. Rev. B **38**, 8358 (1988).
[19]M. A. Gell, D. Ninno, M. Jaros, and D. C. Herbert, Phys. Rev. B **34**, 2416 (1986).
[20]J. S. Nelson, C. Y. Fong, Inder P. Batra, W. E. Pickett, and B. M. Klein, Phys. Rev. B **37**, 10 203 (1988).
[21]M. A. Gell, M. Jaros, and D. C. Herbert, Superlatt. Microstruct. **3**, 121 (1987).
[22]D. M. Bylander and L. Kleinman, Phys. Rev. B **36**, 3229 (1987).
[23]S. H. Wei and A. Zunger, J. Appl. Phys. **63**, 5794 (1988).
[24]S. H. Wei and A. Zunger, Appl. Phys. Lett. **53**, 2077 (1985).
[25]R. Eppenga and M. F. H. Schuurmans, Phys. Rev. B **38**, 3541 (1988).
[26]T. Nakayama and H. Kamimura, J. Phys. Soc. Jpn. **54**, 4726 (1985).
[27]W. Andreoni and R. Car, Phys. Rev. B **21**, 3334 (1980).
[28]N. Sano, H. Kato, M. Nakayama, S. Chika, and H. Teruchi, Jpn. J. Appl. Phys. **23**, L640 (1984).
[29]H. Terauchi, Y. Noda, K. Kamigaki, S. Matsunaka, M. Nakayama, H. Kato, N. Sano, and Y. Yamada, J. Phys. Soc. Jpn. **57**, 2416 (1988).
[30]T. Nakazawa, H. Fujimoto, K. Imanishi, K. Taniguchi, C. Hamaguchi, and S. Sasa, J. Phys. Soc. Jpn. **58**, 2196 (1989).
[31]O. J. Glembocki, B. V. Shanabrook, N. Bottka, W. T. Beard, and J. Comas, Appl. Phys. Lett. **46**, 970 (1985).
[32]O. J. Glembocki, B. V. Shanabrook, N. Bottka, W. T. Beard, and J. Comas, in *Proceedings of The Society of Photo-Optical Instrumentation Engineers Conference on Spectroscopy Characterization Techniques for Semiconductor Technology II* (The Society of Photo-Optical Instrumentation Engineers, Bellingham, WA, 1985), Vol. 524, p. 86.
[33]J. L. Shay, Phys. Rev. B **2**, 803 (1970).
[34]Y. Sasaki, C. Hamaguchi, M. Yamada, and J. Nakai, Rev. Sci. Instrum. **44**, 705 (1973).
[35]D. E. Aspnes and J. E. Rowe, Phys. Rev. B **5**, 4022 (1972).
[36]D. E. Aspnes, Surf. Sci. **37**, 418 (1973).
[37]B. O. Seraphin and N. Bottka, Phys. Rev. **145**, 628 (1966).
[38]H. H. Rosenbrock, Comput. J. **3**, 175 (1960).
[39]O. J. Glembocki and B. V. Shanabrook, Superlatt. Microstruct. **5**, 603 (1989).
[40]J. Bleuse, G. Bastard, and P. Voisin, Phys. Rev. Lett. **60**, 220 (1988).
[41]F. Agulló-Rueda, E. E. Mendez, and J. M. Hong, Phys. Rev. B **40**, 1357 (1989).
[42]E. E. Mendez, F. Agulló-Rueda, and J. M. Hong, Phys. Rev. Lett. **60**, 2426 (1988).
[43]G. Bastard, E. E. Mendez, L. L. Chang, and L. Esaki, Phys. Rev. B **28**, 3241 (1983).
[44]D. A. B. Miller, D. S. Chemla, T. C. Damen, A. C. Gossard, W. Wiegmann, T. H. Wood, and C. A. Burrus, Phys. Rev. B **32**, 1043 (1985).
[45]H. Hazama, T. Sugimasa, T. Imachi, and C. Hamaguchi, J. Phys. Soc. Jpn. **55**, 1282 (1986).
[46]P. Vogl, H. P. Hjalmarson, and J. D. Dow, J. Phys. Chem. Solids **44**, 365 (1983).
[47]K. E. Newman and J. D. Dow, Phys. Rev. B **30**, 1929 (1984).
[48]H. Fujimoto, C. Hamaguchi, T. Nakazawa, K. Imanishi, and K. Taniguchi, J. Phys. Soc. Jpn. **58**, 3727 (1989).
[49]P. Lawaetz, Phys. Rev. B **4**, 3460 (1971).